[CANCER RESEARCH 57, 504–512, February 1, 1997]

Structure and Expression of the Human *FHIT* Gene in Normal and Tumor Cells[1]

Teresa Druck, Piotr Hadaczek,[2] Tie-Bo Fu, Masataka Ohta,[3] Zurab Siprashvili, Raffaele Baffa, Massimo Negrini, Kumar Kastury, Maria Luisa Veronese, David Rosen, Jay Rothstein, Peter McCue, Maria Grazia Cotticelli, Hiroshi Inoue, Carlo M. Croce, and Kay Huebner[4]

Departments of Microbiology and Immunology [T. D., P. H., T-B. F., M. O., Z. S., R. B., M. N., K. K., M. L. V., M. G. C., H. I., C. M. C., K. H.], Otolaryngology [D. R., J. R.], and Surgical Pathology [P. M.], Kimmel Cancer Center, Jefferson Medical College, Philadelphia, Pennsylvania 19107

ABSTRACT

The *FHIT* gene, encoded by 10 exons in a 1.1-kb transcript, encompasses approximately 1 Mb of genomic DNA, which includes the hereditary RCC t(3;8) translocation break at 3p14.2, the *FRA3B* common fragile region, and homozygous deletions in various cancer-derived cell lines. Because some of these genetic landmarks (*e.g.*, the t(3;8) break between untranslated *FHIT* exons 3 and 4, a major fragile region that includes a viral integration site between exons 4 and 5, and cancer cell homozygous deletions in intron 5) do not necessarily affect coding exons and yet apparently affect expression of the gene product, we examined the *FHIT* locus and its expression in detail in more than 10 tumor-derived cell lines to clarify mechanisms underlying aberrant expression. We observed some cell lines with apparently continuous large homozygous deletions, which included one or more coding exons; cell lines with discontinuous deletions, some of which included or excluded coding exons; and cell lines that exhibited heterozygous and/or homozygous deletions, by Southern blot analysis for the presence of specific exons. Most of the cell lines that exhibited genomic alterations showed alteration of *FHIT* transcripts and absence or diminution of Fhit protein.

INTRODUCTION

The *FHIT* gene, spanning the t(3;8) (3p14.2;q24) RCC[5]-associated chromosome translocation, the *FRA3B* common fragile region, and homozygous deletions in cancer cells, is a potential tumor suppressor gene (1) that encodes the human diadenosine triphosphate hydrolase (2). The *in vivo* function of this enzyme, which produces ADP and AMP *in vitro* from the diadenosine substrate, is not known. The 1.1-kb *FHIT* cDNA is encoded by 10 small exons distributed over a genomic locus of about 1 Mb; the t(3;8) break falls between untranslated 5′ exons 3 and 4. The gene overlaps homozygous deletions observed in various cancer cell lines, which often include exon 5, the first protein-coding exon, and usually include portions of the >200-kb intron 5 (1, 3).

The *FHIT* gene is apparently expressed at low levels in most adult tissues but is absent or undetectable by Northern blot in some tumor cell lines with deletions (1). We have previously investigated the integrity of the *FHIT* transcript in small tissue samples from primary tumors by RT from total RNA or mRNA followed by PCR amplification, using primers in exons 1 and 10; this amplification product was then reamplified using primers nested inside the original primers in exons 2 and 9 (1, 4–6). These studies, in parallel with preliminary investigations of the integrity of the *FHIT* genomic locus, suggested that lesions in the *FHIT* genomic locus often resulted in shorter aberrant RT-PCR products and further suggested that aberrant *FHIT* RT-PCR products might be diagnostic of a DNA lesion in cases in which the *FHIT* genomic locus was not or could not be studied in detail. Such aberrant *FHIT* RT-PCR products have been observed in a variety of types of tumors and tumor cell lines, as have *FHIT* genomic lesions, and have been useful in suggesting which cancer cell lines are likely to exhibit alterations within the *FHIT* locus, although Thiagalingam *et al.* (7) have found a lower frequency of involvement of *FHIT* in colon cancer xenografts and have cautioned that nested RT-PCR amplification can produce artifactual aberrant products. In ongoing detailed analyses of the *FHIT* locus, we have undertaken a study to correlate specific *FHIT* locus DNA lesions with their effects on RT-PCR products and Fhit protein expression.

The intron-exon structure of the *FHIT* gene was determined, and intron-exon boundaries sequenced in order to amplify and sequence individual exons that show SSCPs. Ends of cosmids in the *FHIT* contig were sequence tagged (STSs) so that numerous probes throughout the *FHIT* locus could be tested for homozygous deletion. Finally, rabbit antibodies specific for the Fhit protein were generated and used to study Fhit expression in cancer cell lines.

MATERIALS AND METHODS

Cells. Cancer-derived cell lines were obtained from American Type Culture Collection or were kindly donated by Drs. Edward Lattime (RCC cells), Dolly Huang (HK1, CNE1, and CNE2 nasopharyngeal carcinoma cells), Linda Cannizzaro (9944 and 9542 lymphoblastoid cell lines carrying the t(3;8) translocation), or other colleagues and were maintained as described (8). Cos/Fhit-Flag transient transfected cells were previously described (2). The DT36 cell line was established from a laryngeal SCC from a patient who had been treated for multiple head and neck tumors. DT36 cells used in this study had been subcultured between 10 and 20 times.

RNA Extraction, RT, and RT-PCR Amplification. mRNA was isolated from cell lines and tissues after treatment with 4 M guanidinium isothiocyanate, followed by phenol-chloroform extraction and isopropanol precipitation, or total RNAs were prepared using the RNAzol kit (Tel-Test, Inc., Friendswood, Texas), according to the manufacturer's instructions.

RT was performed in 30 μl final volume of 50 mM Tris-HCl, pH 8.3, 75 mM KCl, 3 mM $MgCl_2$, 10 mM DTT, 0.125 mM each dNTP, 500 ng of oligo-dT, 600 units of Moloney murine leukemia virus-reverse transcriptase (Life Technologies, Inc.), 40 units of RNasin (Promega), and 2 μg of RNA. This reaction was incubated at 37°C for 90 min and boiled for 5 min. RT-PCR primers are listed in Table 1.

PCR Amplification. The oligonucleotides for generating PCR products for agarose gel analysis or SSCP analysis were designed using the computer program Oligo 4.0 (National Biosciences) or were taken from the GDB.

PCR amplifications were carried out in 12.5 μl final volume with 100 ng of genomic DNA template, 20 ng of primers, 10 mM Tris-HCl, pH 8.3, 50 mM KCl, 0.1 mg/ml gelatin, 1.5 mM $MgCl_2$, 0.2 mM each dNTP, and 0.5 units of *Taq* polymerase (ABI). The amplifications were performed in a Perkin-Elmer Cetus thermal cycler for 30 cycles of 94°C for 30 s (for denaturation), 57°C

Received 10/7/96; accepted 12/19/96.

The costs of publication of this article were defrayed in part by the payment of page charges. This article must therefore be hereby marked *advertisement* in accordance with 18 U.S.C. Section 1734 solely to indicate this fact.

[1] This work was supported by United States Public Health Service Grants CA51083, CA21124, and CA39860. Kimmel Cancer Center Core Grant CA56336, and a gift from R. R. M. Carpenter III and Mary K. Carpenter.

[2] Present address: Department of Genetics and Pathology, Medical Academy, Al. Powstancow Wlkp. 72, 70-111 Szczecin, Poland.

[3] Present address: Banyu Tsukuba Research Institute, Okubo 3, Tsukuba 300-33 Japan. Phone: 011-81-298-77-2000; Fax: 011-81-298-77-2024.

[4] To whom requests for reprints should be addressed, at Kimmel Cancer Institute, BLSB, Room 1008, 233 South 10th Street, Philadelphia, PA 19107. Phone: (215) 503-4656; Fax: (215) 923-4498.

[5] The abbreviations used are: RCC, renal cell carcinoma; SSCP, single-strand conformation polymorphism; RT, reverse transcription; STS, sequence-tagged site; SCC, squamous cell carcinoma; HNSCC, head and neck SCC; GDB, Genome Data Base; LINE, long interspersed element; YAC, yeast artificial chromosome; GST, glutathione *S*-transferase.

Table 1 *Oligonucleotide primers for PCR amplification*

Primer pairs	Sequences (5′–3′)	Origin
67CF/R	CCCAAATCGTATATGTGCGTG/CTATAGACTAATTGCACTTGG	Cosmid 06 #7 T7 end
i7BF/7B	CCTCCTCATTGTTCCTACAG/TCACTGGTTGAAGAATACAGG	Exon 10
iex9F/R	TTCAAGGAGATCCCAAGG/TGTGCATCCCCATTCTGA	Exon 9
67AF/R	GTCTGCAGAAAGCTATGAGC/TTCCCAAATGCAGCAGGAAC	Cosmid 06 #7 T3 end
59CF/R	TGTCAGTTTGACTCCAGAGC/CATACTCGGAACAATCATGC	Cosmid 05 #9 T7 end
iex8F/R	GGAGTAATTGGGCTTCAT/AGGTTGATGTCATCCCAC	Exon 8
51CF/R	CTCAACTCACTACTGCCACC/TATGGCTTGATCCAGGGAC	Cosmid 05 #1 T7 end
iex7F/016	TGGTCCCCATGAGAATACTA/TTACGGCTCTAACACTGAGG	Exon 7
iex6F/R	GGTCCGAGAGGATTCAAT/TATCAGGAGGAGCAAGCC	Exon 6
51AF/R	TGGCACATGTATTCCCAAGAC/TTCCCAAGTAGCCTGAGAAC	Cosmid 05 #1 T3 end
63A1/A2	TAAGTAACTTGGCCAGAGCT/CGCTGTACAGTGGTAGTCA	Cosmid 63 T3 end
P4A1/A2	GCTGACAAAGGCATAGGCTT/CTGGTTAGTCAGGCTAATGC	Cosmid P4 T3 end
63C1/C2	GTGACTGATTGGCCAACCAA/TCGAAGCTCTTAGATACAGG	Cosmid 63 T7 end
S8A1/A2	AGCTGCCTGTTTCCTCAAC/GAGTGGCTTGTGACAAACTG	Cosmid S8 T3 end
76C1/C2	TTCATTAGGTCAGTTGGTTGAA/CACCGGAAATAATGTTTTCTTCC	Cosmid 76 T7 end
36C1/C2	AATGGATGAACATCCGGAAGT/GGTAACACCACTAGCAATTAGA	Cosmid 36 T7 end
B4A1/A2	ATCTCATGAGCCGACGAGT/CACATGCTTGGAGACATAACTA	Cosmid B4 T3 end
iex5F/R	ATGGCATCCTCTCTGCAA/TTCATTTGGCTGGTTAGG	Exon 5
76AF/R	GTCATTCCTTGGTGCTAG/TCCTGGTTGTAATAGGGC	Cosmid 76 T3 end
B4C1/C2	GCAATATCTGAGAAGCACAGTA/TGAGGCAGCAGTGCACTTA	Cosmid B4 T7 end
U39804F/R	CTGGCCTTATCATTCCTG/TCCAGGGTGGTGACTTCA	Accession #U39804, at nucleotides 11, 262
TGCF/R	AGGGTTAATCAACCAATCCA/TTTGCTATGTGATGAGGCTG	Accession #U39804, at nucleotides 2660, 2971
U39799F/R	GCCAATACCCCAGATAGT/TGGAAAGATGGTTACCTG	Accession #U39799, at nucleotides 123, 332
ex4T7F/R	TGGAGAATGCACACGTTAGC/GGCATATGGTAAGCTCATTGG	Cosmid exon 4 T7 end
iex4F/R	TTGTACCTAGAGCCATCTGG/GGATACTCACAGCAGGTCAA	Exon 4
C7BAF/R	TTGGCTCATAGTAGGTGC/CCTGAGACCTGAAGGATG	Cosmid 7B T3 end
iex3F/R	AGGGTGATACTAGCTGCTTT/TGACTTTAGCCAGTGGCA	Exon 3
ex3T7F/R	TATGTGTGGAGGTCAGAG/AAGAGGACCAAGTGCATG	Cosmid exon 3 T7 end
ex2T3F/R	GGCAATTAACCACATCAG/GTGGAAGAAACAAACCTC	Cosmid exon 2 T3 end
iex2F/R	AGGTACGAGGCACAAGTT/GCAGGTGGTTAAGGAAGT	Exon 2
ex2T7F/R	ATGGGAGACTGCCACAAA/GCCGTTTGGTATTGCCTT	Cosmid exon 2 T7 end
ex1T3F/R	GACCAAGTACCGATGAGTTC/GGTTCGTCAGTTTCATAGACA	Cosmid exon 1 T3 end
UR4/i15′R	CTGCTCTGTCCGGTCACA/GTCGGTGCTTGGGAATTG	Exon 1
ex1T7F/R	TCCTTGTCCTTATCCATT/CCCTTGTTTTACACACGA	Cosmid exon 1 T7 end
UR5/O6	CTGTAAAGGTCCGTAGTG/CTGTGTCACTGAAAGTAGAC	Exon 2 nt 192, exon 9 nt 790

(varied for specific primer pairs) for 30 s (for annealing), and 72°C for 30–60 s (for extension).

SSCP Analysis. The procedure for PCR-SSCP was described previously (9). Samples were amplified by PCR with the appropriate oligonucleotides flanking each exon (Table 1). PCR product (1 μl) was mixed with 10 μl of loading buffer (95% formamide, 10 mM NaOH, 0.05% bromphenol blue, 0.05% xylene cyanol FF) and denatured at 94°C for 5 min. Samples were electrophoresed on a 0.5 × Hydrolink MDE Gel (J. T. Baker, Phillipsburg, NJ) at 5 W for ~18 h.

DNA Sequence Analysis. Representative polymorphic and variant bands (individual alleles) from SSCP gels were cut from the dried gel, reamplified, purified, and sequenced using amplification primers or internal synthetic oligonucleotides. Other PCR products were sequenced after isolation of bands from gels and purification (Qiagen). Sequencing of PCR products was performed using *Taq* DyeDeoxy Terminator Cycle Sequencing Kits (Applied Biosystems, Inc.); reaction products were electrophoresed and recorded on the 373 or 377 DNA sequencer (Applied Biosystems, Inc.). Sequences were analyzed using Genetics Computer Group software (10).

Southern Analyses. High molecular weight DNA from tumor cell lines was extracted using standard methods (8). For Southern blotting, 5 μg of DNA was digested in a 40-μl reaction mix containing 1× restriction buffer, 5 mM spermidine, and 40 units of restriction enzyme (*Bam*HI, *Eco*RV, *Xba*I, or *Hin*dIII; Life Technologies, Inc.). The DNA was electrophoresed on 0.7% agarose gels and blotted to nylon membranes using the Probe Tech 2 Oncor machine. All steps and procedures for DNA depurination, denaturation, and subsequent transfer were performed according to Probe Tech 2 manufacturer's instructions. The membranes were hybridized with a cDNA probe containing exons 1–9 of the *FHIT* gene. The probe was labeled with [α-^{32}P]dCTP by random priming (Life Technologies, Inc.). Both prehybridization and hybridization were at 65°C in 5× saline-sodium phosphate-EDTA, 5× Denhardt's solution, 1% SDS, and 0.1 mg/ml salmon sperm DNA. Hybridized filters were washed in 2× SSC, 0.1% SDS for 15 min, in 0.1× SSC, 0.1% SDS for 15 min at room temperature, and twice for 15 min at 65°C. After being washed, membranes were exposed to Storage Phosphor Screens (Molecular Dynamics, Sunnyvale, CA) and then scanned on the Molecular Dynamics PhosphorImager. Densitometric analysis of exon dosage was performed with the ImageQuant program. Membranes were also exposed to X-ray film to obtain an autoradiographic image of the results.

Rabbit Antibody to GST-Fhit Fusion Protein. Production and purification of the GST-Fhit fusion protein was previously described (2). Rabbits were immunized with ~100 μg of the GST-Fhit fusion protein (in 3 ml total volume, injected s.c. at 500 μl per site, 6 sites per rabbit). The initial injection was with complete Freund's adjuvant. Two weeks later, rabbits were given a booster of incomplete Freund's adjuvant and GST-Fhit antigen. After 4 boosts at 2-week intervals, 5 ml of blood were drawn and the serum was tested for binding to GST-Fhit and the proteolytically cleaved Fhit protein by ELISA and then by immunoblot analysis. The anti-GST-Fhit antibody was routinely used at a 1:1000 dilution for immunoblot analysis of the transiently expressed Fhit-Flag and endogenous Fhit protein.

Immunopurification of Rabbit IgG. The ImmunoPure (A/G) IgG Purification Kit (Pierce) was used to purify anti-Fhit IgG from rabbit sera. First, 5 ml of antiserum was diluted at least 1:1 with ImmunoPure IgG binding buffer and loaded on a Protein A/G column that had been equilibrated with 10 ml binding buffer. When the sample flowed completely into the gel, the column was washed twice with 20 ml of the binding buffer, followed by elution of the bound IgG with 1–2 ml of the ImmunoPure elution buffer. The purified immunoglobulin was applied to a Quick Spin sephadex G-25 column (Boehringer Mannheim) for desalting and exchanging buffer to PBS.

Cell Lysate Preparation and Western Blot Analysis. For analysis of Fhit protein expressed in eukaryotic cells, the transfected Cos1 cells and cells to be tested for expression of endogenous Fhit were washed twice with PBS and scraped into 400 μl of lysis buffer (150 mM NaCl, 1% NP40, 2 mM EDTA, 1 mM DTT, 50 mM Tris, pH 8.0, 10 μg/ml each of chymostatin, leupeptin, aprotinin, and pepstatin, 1 mM phenylmethylsulfonyl fluoride), sonicated for two 30-s pulses at a setting of 6.0 using Sonicator XL2020 (Heat Systems, Inc.) and centrifuged for 10 min at 15,000 × *g*. After protein concentration was measured, ~50–100 μg of total cellular protein were mixed with 5× loading buffer and denatured for 3–5 min at 90°C prior to being loaded on a 12% SDS-PAGE gel. After SDS-PAGE, the gel was blotted and the membrane blocked in 5% dried milk in TBST buffer (10 mM Tris-HCl, pH 8.0, 150 mM NaCl, 0.05% Tween 20) for 1 h at room temperature, followed by three 10-min washes in TBST buffer and incu-

bation for 1–2 h at room temperature with anti-Fhit IgG (1:500–1:2000 dilution). After repeated washes in TBST, the blot was incubated for 1 h with the secondary antibody, antirabbit immunoglobulin labeled with horseradish peroxidase (Amersham) diluted 1:2000 in TBST; TBST buffer washes followed. The signal was detected using the ECL system (Amersham) as described by the manufacturer.

RESULTS AND DISCUSSION

Extent of Homozygous Deletions within *FHIT* in Cancer-derived Cell Lines. At the time of previous reports describing the *FHIT* clones and attendant homozygous deletions (1, 3), the intron sequences surrounding some of the *FHIT* exons had not yet been determined. Cosmids encompassing each of the exons were isolated as described previously (1) by screening cosmid libraries, prepared from individual YAC clones, with *FHIT* cDNA probes. Exon-intron boundary sequences were obtained by sequencing into introns on cosmid templates using forward and reverse oligonucleotide primers within the appropriate exons for each cosmid (Genbank accession numbers U76262–U76272).

Oligonucleotide primers were then designed flanking each exon so that each exon, with intron flanking sequences, could be amplified for SSCP analysis and sequencing of polymorphic or variant bands and for detection of homozygous loss of specific exons (GDB locus names for primer pairs, *D3S4460E–4469E*). For exon 1, we were not able to design a forward 5′ primer that would, in combination with an intron 1 primer, reproducibly amplify in reactions with human DNA template. Thus, for amplification of exon 1 we have placed the forward primer at the 5′ end of the cDNA and the reverse primer in intron 1. Similarly, the forward primer for amplification of exon 10 is within intron 9, but the reverse primer is within exon 10, excluding ~200 bp of the 3′ end of the exon. Cosmid ends were also sequenced (Genbank accession numbers U76273–U76295) with vector primers and sequence tagged (GDB locus names *D3S4459* and *D3S4470–4490*) for amplification from human DNA templates. At one end of cosmid cx3, which includes exon 3, there are extensive sequences homologous to human LINE families, which precluded design of unique oligonucleotide primers. Oligonucleotide primers for amplification of cosmid insert end sequences, individual exons, and other STSs, listed in Table 1, were used to search for homozygous deletion of portions of the *FHIT* locus and *FRA3B* in a panel of cancer cell lines, by PCR amplification, using each primer pair on DNA templates from cancer cells.

We began our search for homozygous deletions using cell lines first shown by Lisitsyn *et al.* (11) to exhibit loss of the BE758-6 marker; these included mostly colon cancer cell lines and a breast tumor cell line. We also tested cancer-derived cell lines of other cancer types that were known to exhibit loss of heterozygosity on 3p, *e.g.*, RCC, which we have shown to lose heterozygosity at high frequency in 3p14.2 (9, 12). Cell lines that we have studied for loss of numerous markers within the *FHIT* locus are shown in Table 2 with an illustration of markers that we find homozygously deleted. *FHIT* exon 5, which is not far centromeric of the BE758–6 marker isolated by Lisitsyn *et al.* (11) and which is near the heart of the *FRA3B* region (1, 13–17), is the most consistently deleted of the protein-coding exons, whereas the RCC cell line RC48 has lost both copies of exons 8–10. Some of the cell lines, such as Siha, CNE1 (a nasopharyngeal carcinoma cell line, not shown), and Kato 3, exhibit homozygous deletions that do not include *FHIT* exons. Other cell lines have retained all or most tested markers (Colo320, RC49, DT36, LNCaP, HOS). The meaning of apparent loss of a single locus from a total of more than 50 tested (not all shown) is not clear. Loss of one locus could be due to polymorphism; therefore, we do not necessarily consider it a DNA lesion unless we find at least two contiguous markers absent. Note that Siha was missing a contiguous marker in intron 4 (not shown). It is possible that the deletion in Siha is near the previously described HPV16 integration site (15), which we have determined to be in intron 4. A striking feature of the types of homozygous deletions observed is their complexity; *e.g.*, the LS180 and AGS cell lines appear to have lost at least three separate regions, and other cell lines have lost more than one region within the *FHIT* locus, as reported previously (3). Additionally, in spite of multiple repetitions of primer and template combinations, some markers, reproducibly, were very faintly amplified (note F+ and VF+ in Table 2). These faint products could be due to homozygous deletion of the indicated locus in most of the cells within a cell line or to polymorphism in the human genome leading to mismatches in one or more of the primers.

The observation of multiple separate homozygous deletions within the *FHIT* locus in LS180, AGS, and MB436 cell lines prompts questions concerning their origin. Why should AGS cells have lost the exon 3 region, retained exon 4, and lost exon 5? Presumably, once exon 5 was lost and produced a selective advantage, later loss of exon 3 could not produce a further tumor growth advantage, unless there are multiple gene targets in the region. If exon 3 was lost first and caused a diminution in translation of the Fhit protein, then later loss of exon 5 could produce a further advantage by elimination of Fhit. Another possibility is that the mechanism of breakage at *FRA3B* frequently allows multiple gaps to form on the same chromosome 3p, which when repaired leave multiple deletions simultaneously.

The observation of faint PCR amplification products (F+) observed mainly in the 5′ end of the *FHIT* gene in RC49 and DT36, for example, suggests the possibility that subpopulations of cells in these cell lines may be missing portions of the *FHIT* gene, an indication that some of these cell lines are not clones; *i.e.*, either the tumors were heterogeneous for *FHIT* deletions and have remained so during culture, which would suggest that *FHIT* alteration may not give a growth advantage in culture, or the established cells may have been clones at first but have been sustaining *FHIT* hits in culture, some of which have been selected for by *in vitro* growth.

Alterations of *FHIT* Exons Detected by Southern Blot Analysis. The deletions for some of these cell lines have been partially described previously (1, 3, 11) but with the availability of sequences surrounding each of the exons and more extensive intron sequences (Table 1), we have now tested for presence of each exon and more intron regions as shown in Table 2. To characterize more fully the genomic alterations of the *FHIT* gene, we performed Southern blot analysis of DNAs from human tumor cell lines. To look for *FHIT* gene rearrangements or deletions we used three restriction enzymes (*Bam*HI, *Eco*RV, and *Xba*I) that do not cut within the cDNA and one enzyme (*Hin*dIII) that cuts only once, at 3 bp from the end of exon 1. To establish sizes of restriction fragments for individual exons, restriction maps of YAC and cosmid clones containing portions of the *FHIT* gene were constructed (data not shown) using the same enzymes and full-length and partial cDNA probes or exon probes. Our studies revealed a number of alterations in the cancer lines examined. *Bam*HI digestion and hybridization to near-full-length cDNA resulted in a group of fragments of high molecular weight representing exons, as illustrated in Fig. 1*A*. Of 13 cancer cell DNAs cleaved with *Bam*HI, 8 showed alterations that apparently corresponded to losses of different *FHIT* exons. The two most commonly observed abnormalities were absence or reduction of the exon 5 fragment (4 of 13 cell lines, summarized in Table 3) and absence or diminution of the exon 3 or 4 band (5 of 13 cell lines), the exons that flank the t(3;8) translocation (see Fig. 1*A*, *Lanes 3–5, 7,* and *9*). Exon 5 fragment losses seen with *Bam*HI (Fig. 1*A*, *Lanes 4* and *8*) were confirmed by *Eco*RV cleavage (see Fig. 1*B*, *Lanes 6* and *7*). The AGS cells (Fig. 1*A*, *Lane 7*), in

Table 2 *Delineation of FHIT locus homozygous deletions in cancer cells*

DNA from cell lines listed across the top of the table served as the template for PCR amplification using oligonucleotide primer pairs (listed on the left with markers ordered from telomeric to centromeric, top to bottom), for *FHIT* region microsatellite and STS markers, cosmid human insert ends, and *FHIT* exons. Results for a subset of the most informative markers are shown. Similar types of cancer cell lines are grouped together: colon carcinoma cell lines, Colo320, HT29, LS180, and SW480; gastric carcinoma cell lines, AGS and Kato3; cervical carcinoma cell lines, HeLa and Siha; and RCC cell lines, RC48 and RC49. Other cancer types are represented by single cell lines: HKI, nasopharyngeal carcinoma; MB436, breast carcinoma; DT36, squamous cell carcinoma of head and neck; and HOS, human osteosarcoma. Partial results of tests for homozygous deletions in some of these cell lines were reported previously (3). The *FHIT* exon results are in bold print and positions of important *FHIT* region landmarks are indicated by the lines between exon 3 and *D3S1481* (t(3;8) break), between sequence-tagged cosmid ends EX4T7 and B4 (HPV16 integration site), and between exon 5 and B4A cosmid end (a fragile site of the *FRA3B* region). We have positioned these landmarks by PCR amplification of cosmid, hybrid, and YAC DNA templates using primer pairs described previously or designed based on published sequences (1, 15, 16). Note that for cosmids cX3, 2 and 1, orientation is unknown; therefore, the order of these cosmid ends could be reversed, relative to the respective exons. The shaded areas highlight apparent homozygous deletions. For HeLa cells, we have tested four DNA preparations; one preparation seemed to show a homozygous deletion surrounding exon 5, but other preparations suggested that this depended on the dilution of DNA tested. Therefore, we believe that exons 3 and 4 or nearby markers are present in reduced amount but are not entirely absent in the HeLa DNAs tested.

	Cell line															
Marker	Colo320	LoVo	HT29	LS180	SW480	AGS	Kato 3	MB436	Hela	Siha	HK1	RC48	RC49	DT36	LNCaP	HOS
67C	+	+	+	+	+	+	+	+	+		+	+	+	+		+
Exon 10	+	+	+	+	+	+	+	+	+		+	−	+	+		+
Exon 9	+	+	+	+	+	+	+	+	+		+	−	+	+		+
67A	+	+	+	+	+	+	+	+	+		+	−	+	+		+
59C	+	+	+	+	+	+	+	+	+		+	−	+	+		+
Exon 8	+	+	+	+	+	+	+	+	+		+	−	+	+		+
51C	+	+	+	+	+	+	+	+	+		+	−	+	+		+
Exon 7	+	+	+	+	+	+	+	+	+		+	+	+	+		+
Exon 6	+	+	+	+	+	+	+	+	+		+	+	+	+		+
51A	+	+	+	+	+	+	+	+	+		+	+	+	+		+
D3S2977		−	+	+	+	−	+	+	+	+	+				+	
63A	+	−	−	−	+	−	−	+	+	+	+	+	+	+	+	+
P4A	+	−	−	+	−	−	−	−	+	+	+	+	+	+	+	+
63C	+	−	−	+	−	−	−	−	+	+	+	+	+	+	+	+
S8A	+	−	−	+	−	−	−	−	+	+	+	+	+	+	+	+
AP4/5	−	−	−	−		−	−	+	+	+	−	+	+	+		+
76C	+	−	−	−	−	−	−	−	+	+	−	+	+	+	+	+
BE758	+	−	−	−	−	−	+	−	+	+	−	+	+	+	+	+
36C	+	−	−	−	−	−	+	−	+		−	+	+	+	+	−
D3S1300	+	−	−	−	−	−	+	−	+	+	−	+	+	+		+
B4A	+	−	−	−	−	−	+	−	+	+	−	+	+	+	+	+
Exon 5	+	−	−	+		−	+	−	+	+	−	+	+	+	+	+
76A	+	−	−	+	−	−	+	−	+	F+	−	+	+	+	+	+
B4C	+	−	−	−	−	−	+	−	+	−	−	+	+	+	+	+
U39804	+	+	+	+	+	+	+	+	+	+	+	+	+	+	+	+
TGCF/R	+	+	+	+	+	−	+	+	+	+	+	+	+	+	+	−
U39799	+	+	+	+	+	−	+	+	+	+	+	+	+	+	+	VF+
EX4T7	+	+	+	+	+	+	+	+	+		+	+	VF+	VF+		+
D3S4260	+	+	+	+		+	+	+	+		+	+	+	+	+	+
IA6G/H	+	+	+	+		+	+	+	+		+	+	+	+	+	+
Exon 4	+	+	+	+	+	+	+	+	+	+	+	+	+	+	+	+
c7BAF/R	+	+	+	+	+	+		+	+		+	+	+	+	+	+
D3S1388	+	+	+	+	+	−	+	+	+		+	+	+	+		+
D3S1481	+	+	+	+	+	−	−	+	+		+	+	+	+	+	+
Exon 3	+	+	+	+	+	−	+	+	+	+	+	+	VF+	+	+	VF+
EX3T7	+	+	+	+	+	−	+	+	+			+	+	+		+
EX2T3	+	+	+	+	+	+	+	+	+	+	+	VF+	+	+	+	+
Exon 2	+	+	+	+	+	+	+	+	+	+	+	F+	+	F+	+	F+
EX2T7	+	+	+	+	+	+	+	+	+		+	F+	F+	F+		+
EX1T3	+	+	+	+	+	+	+	+	+		+	+	F+	F+		+
Exon 1	+	+	+	+	+		+	+	+		+	+	+	+	+	+
EX1T7	+	+	+	+		+	+	+	+		+	+	+	+	+	VF+
D3S1312	+	+	+	+	+	+	+	+	+		+	+	+	+	+	+

addition to exon 5 loss, showed absence of the exon 4 and exons 6, 7 fragments and three rearranged bands; with *Hin*dIII, absence of exon 5, diminution of the exons 3, 7 band, and a rearrangement were observed (not shown). The RCC cell line RC48 (Fig. 1*A*, *Lane 2*) clearly showed absence of *Bam*HI fragments corresponding to exons 6, 7 and exons 2, 9. Absence of exon 8 and 9 fragments in this cell line was confirmed by results of Southern blot analysis after cleavage with the three other enzymes (Fig. 1, *B*, *Lanes 2* and *9*, and *D*, *Lane 2*). RC49 DNA cut with *Eco*RV revealed one additional 2.3-kb fragment (Fig. 1*B*, *Lane 1*), which derives from rearrangement of one allele of exon 8 as determined using individual exon probes (not shown); rearrangement was not observed with other enzymes. Cleavage of DNAs with *Xba*I resulted in well-separated, high molecular weight fragments, but fragments for several exons were in the same size class; for example, exons 2, 6, and 7 all hybridized to 7.7-kb bands (see summary of exon placement in Fig. 1*D*) and could not be resolved as distinct fragments; exons 6 and 7 may actually be contained in one *Xba*I fragment because they are only separated by 2.5 kb (determined by interexon PCR, data not shown). Additionally, exons 5 and 8 comigrated at 5.7 kb (Fig. 1*D*). Thus, with *Xba*I digestion of RC48 DNA, it is clear that the 4.8 kb exon 9 band is missing (Fig. 1*D*, *Lane 2*) but absence of exon 8 (observed for RC48 after *Eco*RV cleavage; Fig. 1*B*, *Lane 2*) is obscured by presence of exon 5. Densitometric analysis was performed to show the relative intensity ratio between bands for some cell lines. For example, in Kato 3 DNA (Fig. 1*D*, *Lane 4*), the 7.7-kb band is less intense when compared to the 5.1-kb exon 1 band (~0.5:1) relative to the 7.7 kb:5.1 kb ratio in other lanes (~1:1). This change in ratio probably means that one or more of exons 2, 6, and 7 is missing or reduced in the Kato 3 cell line. The conclusions we have drawn from the Southern blot analysis are summarized in Table 3 for all the cell lines.

The *Bam*HI and *Xba*I digestions revealed a possible polymorphism

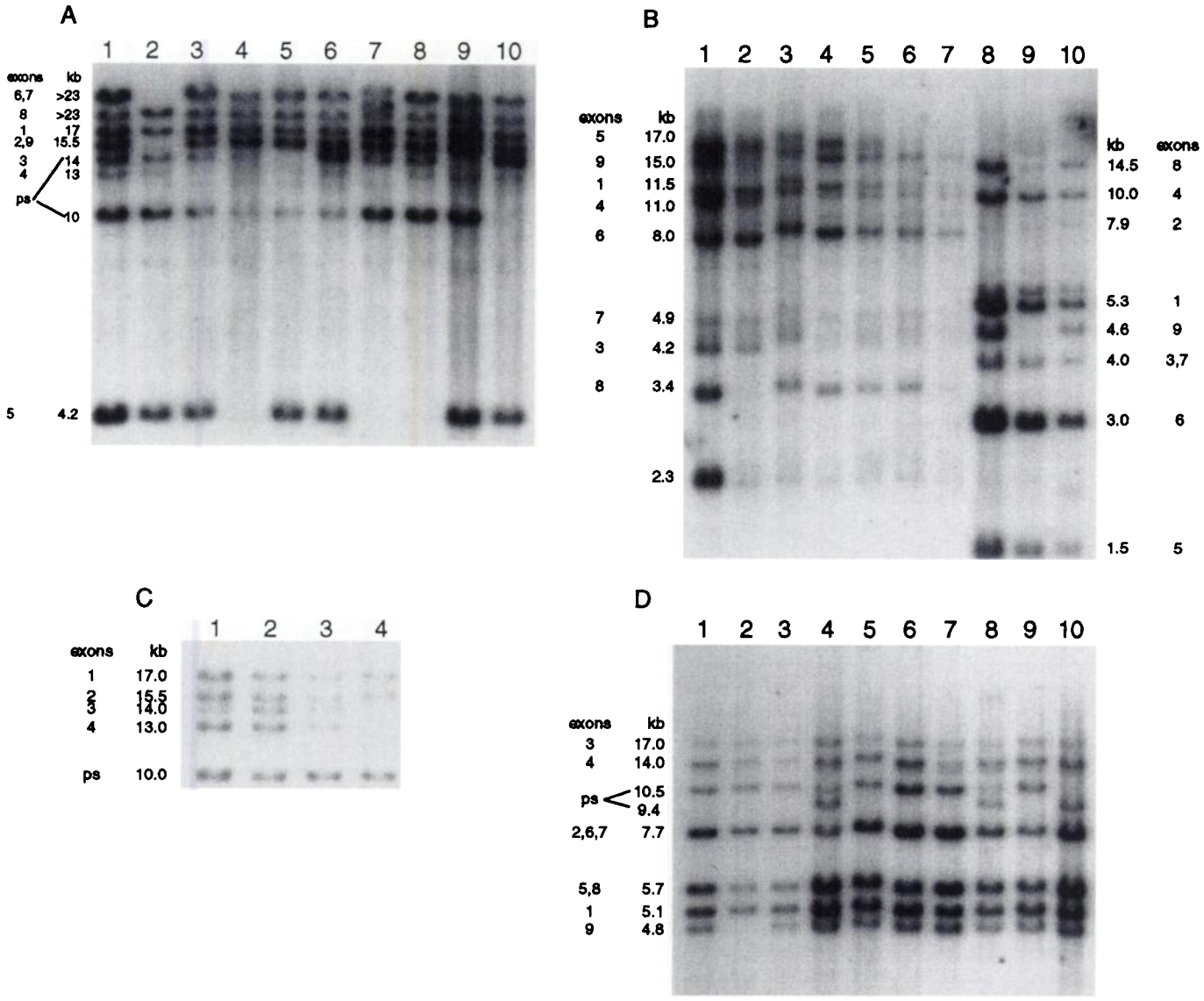

Fig. 1. Southern blot analysis of the *FHIT* gene in human tumor cell lines. Hybridization of *FHIT* cDNA probes to enzyme-cleaved DNAs from human cell lines. *A*, *Bam*HI-digested DNA (5 μg/lane) from RC49 (*Lane 1*), RC48 (*Lane 2*), Colo320 (*Lane 3*), LoVo (*Lane 4*), HeLa (*Lane 5*), DT36 (*Lane 6*), AGS (*Lane 7*), HK1 (*Lane 8*), LNCaP (*Lane 9*), and A549 (*Lane 10*). *B*, *Lanes 1–7*, *Eco*RV cleaved DNA from RC49, RC48, TL9542, HeLa, DT36, LoVo, and HK1; *Lanes 8–10*, *Hin*dIII cleaved RC49, RC48, DT36 DNAs. *C*, Hybridization with a cDNA probe containing exons 1–4 of the *FHIT* gene to *Bam*HI-cleaved DNAs from cell lines Colo320 (*Lane 1*), 9944 (*Lane 2*), RC48 (*Lane 3*), and HeLa (*Lane 4*). *D*, *Xba*I-digested DNAs from RC49 (*Lane 1*), RC48 (*Lane 2*), Colo320 (*Lane 3*), Kato 3 (*Lane 4*), TL9542 (*Lane 5*), Siha (6), HeLa (*Lane 7*), DT36 (*Lane 8*), K562 (*Lane 9*), and A549 (*Lane 10*). The membranes shown in *A*, *B*, and *D* were hybridized to a *FHIT* probe containing exons 1–9. The sizes of specific restriction enzyme fragments are shown beside each panel, and exons contained in specific restriction fragments are indicated. *ps*, pseudogene of exons 1–3, which exhibits polymorphisms, as shown with *Bam*HI and *Xba*I.

detected by hybridization to the near-full-length *FHIT* cDNA (Fig. 1*A*, *Lane 6* shows both alleles; *Lane 10*, the upper allele only overlapping the exon 3 fragment; *Lanes 1–5* and *7–9*, the lower allele only; in Fig. 1*D*, the polymorphic *Xba*I fragments do not overlap the *FHIT* exon fragments so the alleles are seen more clearly). The polymorphic locus was cloned from a genomic library, sequenced, and identified as a pseudogene of exons 1, 2, and 3 that maps to chromosome region 1p (data not shown).

It was not always possible to deduce the actual structure of the *FHIT* loci remaining in some of the cancer cell lines, even by combining the results of the PCR analysis for homozygous deletion (Table 2) with the Southern blot results. For RC48, the *Bam*HI digestion (Fig. 1*A*, *Lane 2*) originally suggested that exons 6 and 7 might be homozygously deleted and probably exon 9 as well. However, the *Eco*RV digestion indicated that exon 8 and 9 were missing (Fig. 1*B*, *Lane 2*). The *Hin*dIII digestion showed absence of the exon 9 fragment, whereas near the exon 8 fragment position there was a faint band of the size of exon 8 and an apparent rearranged band above (Fig. 1*B*, *Lane 9*). The *Xba*I digestion of RC48 (Fig. 1*D*, *Lane 2*) revealed the absence of the exon 9 fragment and a relatively fainter exon 5/8 fragment relative to the exon 1 fragment. Combining these results with the PCR amplification results in Table 2, the best interpretation is that the homozygous deletion begins in intron 7, includes the normally occurring *Bam*HI site flanking exon 7, and extends past exon 10; thus, the exon 6/7 *Bam*HI fragment is now smaller and appears to be the same size as the exon 8 fragment. The rearranged *Hin*dIII fragment (Fig. 1*B*, *Lane 9*) may represent a rearranged exon 7. The Kato 3 cell line is another interesting example, for which PCR amplification of *FHIT* locus markers (Table 2) indicated homozygous deletion of a telomeric portion of intron 5. The Southern analysis indicated relatively fainter *Xba*I 7.7-kb fragments representing exons 2, 6, and 7, suggesting that some cells in the Kato 3 population were probably missing exon 6 or 7 and showing that the Kato 3 population is heterogenous; exon 6 and 7 are clearly present, as illustrated by the

Table 3 *Summary of characterization of the FHIT gene in cancer-derived cell lines*

Cell line	Origin	RT-PCR	Exon SSCP or PCR	Southern blot analysis with cDNA and exon probes				Protein
				*Bam*HI	*Eco*RV	*Xba*I	*Hind* III	
293	Kidney	N[a]	N	N	NT	NT	NT	+++
RC49	RCC	N	N	N	Rearranged e8	N	N	+
RC48[b]	RCC	−	−e8,9,10	−e6,7,9 bands	−e8,9 bands	−e8,9 bands	−e8,9 bands	−
Colo320	Colon ca	N	N	e4 band reduced	e4 band reduced	e3,4 bands reduced	NT	+
LoVo[b]	Colon ca	ab	−e5	−e4,5 bands	−e5 band	NT	NT	NT
Kato 3[b]	Gastric ca	ab	N	N	N	e2,6,7 band reduced	NT	−
AGS[b]	Gastric ca	ab	−e3,5	−e4,5,6,7 bands, rearranged bands	NT	NT	−e5 band, rearranged bands	−
Hela	Cervical ca	N,ab	N	e3,4 bands reduced	e3,4 bands reduced	e3,4 bands reduced	NT	+
Siha[b]	Cervical ca	ab	NT	e5 band reduced	NT	NT	e5 band reduced	−
DT36	HNSCC	ab	faint e2	N	N	N	N	−,V
U2020	SCLC	N	N	N	N	NT	NT	++
HKI[b]	NPC	−	−e5	−e5 band	−e5 band	NT	NT	−
LNCaP	Prostate ca	N,ab	NT	e3 band reduced	NT	NT	NT	+
HOS	Osteosarcoma	N,ab	faint e3	N	e7 band reduced	NT	NT	NT
9944, 9542[c]	T lymphoblastoid	N	N	N	N	N	NT	ND

[a] N, normal; ab, aberrant; e, exon; NT, not tested; ND, not detected; ca, carcinoma; −, minus; NPC, nasopharyngeal carcinoma.

[b] Cell lines with homozygous deletions in the *FHIT* locus; note that in cancer cell lines with homozygous deletions Fhit expression was not detected.

[c] 9944 and 9542 are lymphoblastoid cell lines established from lymphocytes of two individuals carrying the RCC-associated t(3;8)(p14.2;q24) chromosome translocation. 293 is an adeno 5 T-antigen transformed kidney cell line.

PCR amplification (Table 2) and other Southern blots (not shown). Other indications of heterogeneity in these cancer cell lines are that HeLa cells show nearly absent exon 3 and 4 fragments (Fig. 1, *A*, *Lane 5*; *B*, *Lane 4*; *C*, *Lane 4*; and *D*, *Lane 7*) but exons 3 and 4 are amplified from HeLa DNA (Table 2); LoVo cells are missing the *Bam*HI exon 4 band (Fig. 1*A*, *Lane 4*); and LNCaP exhibits absence of the exon 3 band (Fig. 1*A*, *Lane 9*), but these exons are present in both by PCR amplification. Some of the apparent absences may be due to undetected rearrangements or polymorphisms. Because of this complexity, it is not always possible to say what the genomic alteration is, even with both PCR amplification and Southern results. For example, HeLa cells must be a mixed population, with most cells missing exons 3 and 4 but some cells retaining these exons. This suggestion of lack of clonality of HeLa cells is surprising, although the HeLa DNA we used was not from a specific HeLa cell clone. Clearly, cell lines can be heterogenous for *FHIT* deletions (18), even at very early passage, showing that the tumors are heterogenous. This tumor heterogeneity is the likely explanation for presence of normal and abnormal *FHIT* RT-PCR products in individual tumors and cell lines, but the meaning of this heterogeneity is not clear. It is possible that some heterogeneity is introduced into the cell lines by the original tumor heterogeneity, but it is also possible that breaks in the *FRA3B* occur during tissue culture passage. However, we have no reason thus far to suppose that *FHIT* deletion imparts an *in vitro* growth advantage. Thus, complete understanding of the genomic rearrangements and deletions will probably require subcloning of the cells of certain cell lines and much more detailed molecular analyses. Nevertheless, our analysis thus far has uncovered some genomic alterations in the *FHIT* locus in most of the cell lines selected for examination.

SSCP and RT-PCR Analyses. The forward and reverse primer pairs for exons were also used to amplify each *FHIT* exon, with various lengths of flanking intron sequences, from 26 cancer-derived cell lines. Labeled amplified products were separated on polyacrylamide gels, autoradiographed, and analyzed for occurrence of variant bands. Variant bands, *i.e.*, SSCPs, were cut from the gels, reamplified, purified, and sequenced. Examples are shown in Fig. 2 and results are summarized in Table 4. Lymphocyte DNAs from 47 donors were simultaneously analyzed for all *FHIT* exons to identify apparent common and rare polymorphisms. If a tumor cell line showed a polymorphic sequence not seen in any other cell, it was considered a variant; types of variants and polymorphisms observed are listed in Table 4.

Cell lines for which all exons were studied are as follows: lung carcinomas, U2020, U1285, H69, and A549; colon carcinomas, Colo320, LoVo, HT29, LS180, and SW480; gastric carcinomas, Kato 3, RF48, and AGS; nasopharyngeal carcinomas, HK1, CNE1, and CNE2; cervical carcinoma, HeLa; breast carcinoma, MDA-MB-436; prostate carcinoma, LNCaP; HNSCC, DT36; RCCs, RC48, RC17, and RC49; ACHN, RC8; pre-B cell leukemia, 697; ovarian carcinoma, CAOV3; and transformed kidney cell line, 293. In addition, DNA from lymphocytes of a t(3;8) carrier was tested. Only results for cell lines for which loss, reduction, polymorphism, or variation was found for at least one exon are included in Table 4. Most of the polymorphisms and variants were sequenced. The findings summarized in Table 4 show that there is a reasonable frequency of polymorphism detected for exons 7, 8, and 10 and a few for exon 4. The polymorphisms are found mostly in introns, with a few silent changes in the protein-coding region. PCR-SSCP also confirmed previous PCR results that had suggested absent or nearly absent exons, as for RC48 exons 8–10. The absence of missense, nonsense, and frameshift mutations in the *FHIT* alleles and exons remaining in the tumor cells is consistent with the suggestion that deletions and rearrangements affecting the *FHIT/FRA3B* locus may occur at a higher frequency than mutations and will thus be the likely mechanism of inactivation of the *FHIT* gene or other possible genes in the *FRA3B* region.

Other notable results of the PCR-SSCP analysis are as follows: exon 2 was poorly amplified from the DT36 HNSCC cell line (Fig. 2, *Lane 8*), in agreement with the results of PCR amplification experiments summarized in Table 2; in addition, exons 2 and 3 were not robustly amplified from RCC cell lines RC48 and RC49 (Fig. 2, *Lanes 1* and *2*) in the SSCP analysis, in agreement with the faint or very faint amplification of the exon 2 region (for RC48) and exon 3 (for RC49) observed by PCR amplification and agarose gel analysis (Table 2); exon 5 was absent from LoVo cells (Fig. 2, *Lane 7*) as shown by Southern blot experiments; both exons 5 and 6 for Kato 3 (Fig. 2, *Lane 4*) were less strongly amplified than other Kato 3 exons, in agreement with the suggestion from Southern analysis described above that exon 6 may be missing in a subpopulation of Kato 3 cells (or exon 6 may be missing from one *FHIT* allele in most or all of Kato 3 cells; possibly the same is true of exon 5 on the other allele); exons 8, 9, and 10 are not amplified from RC48 (Fig. 2, *Lane 1*) in agreement with results of Southern analysis.

We had previously briefly described RNA expression of the *FHIT* gene in some of these cancer cell lines (1); because steady state levels of *FHIT* RNA are low, *FHIT* expression in cancer cells has mainly been analyzed by nested RT-PCR amplification reactions (1, 4, 6, 18).

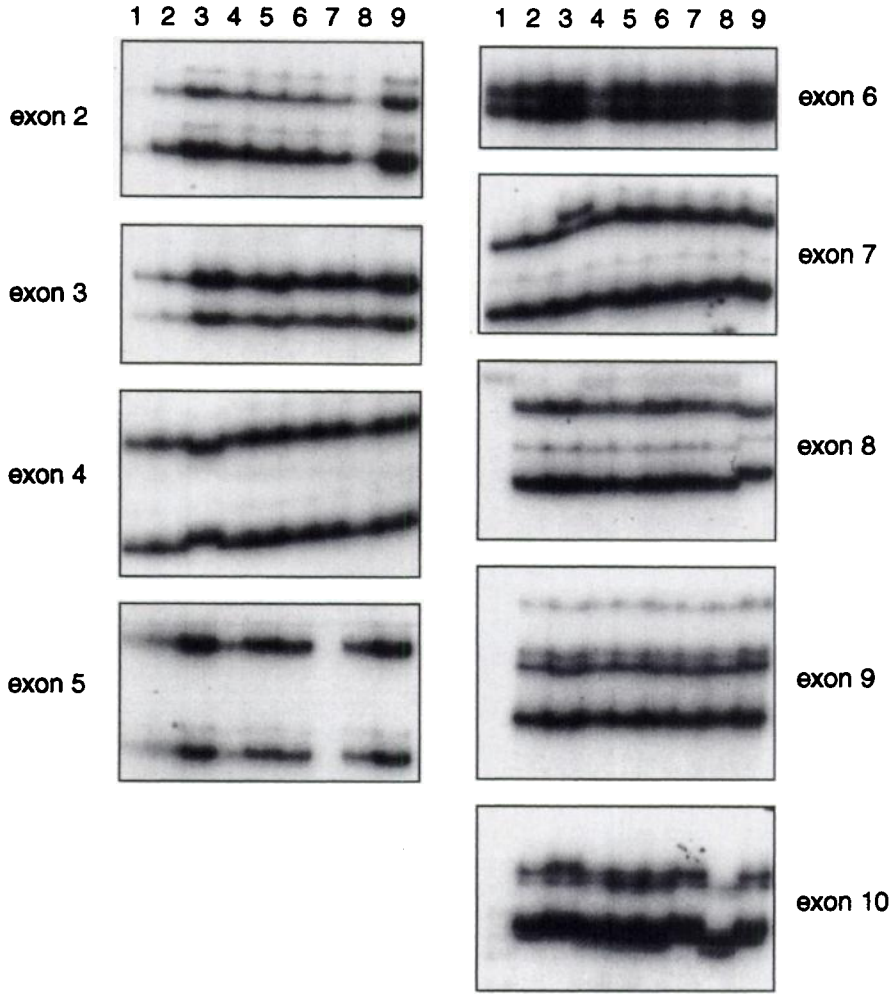

Fig. 2. SSCP analysis of *FHIT* exons. Exons were amplified using the flanking intron primers shown in Table 1, and the labeled amplification products were separated on nondenaturing PAGE gels at room temperature. The gels were dried and autoradiographed as shown for exons 2–10 for cell lines RC48 (*Lane 1*), RC49 (*Lane 2*), HeLa (*Lane 3*), Kato 3 (*Lane 4*), 697 (a human pre-B cell leukemia; *Lane 5*), 9944 (a lymphoblastoid line from a t(3;8) carrier; *Lane 6*), LoVo (*Lane 7*), DT36 (*Lane 8*), and DNA from a YAC clone containing the relevant region of the *FHIT* locus (*Lane 9*). Note that the RC48 DNA (*Lane 1*) is missing exons 8, 9, and 10. Although exons 2 and 3 are not intensely labeled for RC48, all of these results have been reproduced at least three times; note also that LoVo is missing exon 5 and that DT36 is very faint for exon 2.

Results of the RT-PCR amplification for a number of cancer cell lines are shown in Fig. 3.

Others have suggested (7), and we and our colleagues have noted, that such nested-PCR amplification reactions are occasionally susceptible to apparent artifacts. Examples are: (*a*) sometimes the RT-PCR products from lymphocytes of apparently normal donors show amplification of normal and aberrant sized products; this seems to occur when the amount of the beginning RNA is very low and/or of questionable quality; (*b*) when RT products from cell lines that exhibit both normal and aberrantly sized products are amplified in three or four separate experiments, the aberrant bands may not be of identical size in every experiment; and (*c*) RT-PCR products from cells exhibiting only aberrant products may not be identical from one experiment to another, but cells with only aberrant bands consistently give only aberrant bands. Some examples of products of nested RT-PCR amplification from RNA of relevant cancer cell lines are shown in Fig. 3. Our interpretation of the aberrant bands currently is that they are an indication of a DNA lesion in the *FHIT* locus. In cases for which we

Table 4 *Summary of SSCPs in cancer cell lines*

Exon	Source of DNAs: Lymphocytes (47 individuals)	Source of DNAs: Cancer cell lines (26 lines)
1	No variants	No variants
2	Rare polymorphism, 97 bp into intron 2, G → T; present in two cases, both heterozygotes	Missing or faintly positive in DT36
3	No variants	Missing in AGS; very faint in U1285 and HT29
4	Six cases heterozygous for alleles *A* and *C* (*C* not sequenced); two cases heterozygous for alleles *A* and *V* (where *V* is different for the two; one *V* defined as −41 bp G → A); one case heterozygous for alleles *A* and *B*	A549 homozygous for C; Hela homozygous for allele *B* (T → A, 16 bases into intron 4); ACHN, A, B heterozygote; CNE2, very faint product
5	No variants	Missing in LoVo, HT29, LS180, SW480, MDA-MB436, HK1, AGS; very faint in CNE2
6	Three *A*, *B* heterozygotes; *B* not defined	No variants
7	Nine *A*, *B* heterozygotes; two *B* homozygotes; *B* allele is C264T, a silent change	One *A*, *B* (Hela); two *B* homozygotes (U2020 and SW480); AGS, *V* allele (T252C, silent)
8	Twelve *A*, *B* heterozygotes, three *B* homozygotes; *B* allele is T294C, silent	Missing in RC48; two *B* homozygotes (HK1 and RC17)
9	Two *A*, *B* heterozygotes, two *B* homozygotes; *B* is T → *A* 17 bp upstream of e8	Missing in RC48; four *B* homozygotes (DT36, CNE1, CNE2, LoVo); one *A*, *B* heterozygote
10	Seven *A*, *B* heterozygotes, two *B* homozygotes; *B* is defined as a deleted C in run of seven C's at 870 bp	Missing in RC48; four *A*, *B* heterozygotes (Kato 3, Colo320, LS180, 697), one *B* (DT36)

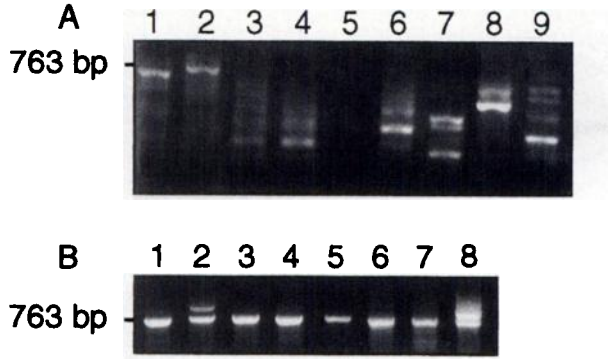

Fig. 3. RT-PCR analysis of *FHIT* expression. RNAs were reverse transcribed using a polydeoxythymidylic acid primer and amplified using outer primers (primers UR4 and 7B in exons 1 and 10) for 30 cycles. The products of the first amplification were then amplified using inner primers, UR5 and O6, in exons 2 and 9. All RT products were also amplified using primers for β actin to ensure integrity of the template cDNAs (not shown). After the second amplification round, one-half of the amplified products were run in agarose-ethidium bromide gel, and the products visualized and photographed. *A*, nested RT-PCR products from LS180 (*Lane 1*), Colo320 (*Lane 2*), CNE1 (*Lane 3*), CNE2 (*Lane 4*), HK1 (*Lane 5*), LoVo (*Lane 6*), Kato 3 (*Lane 7*), HeLa (*Lane 8*), and colon carcinoma CCL 235 (*Lane 9*). *B*, nested RT-PCR products from lymphocytes of four donors (*Lanes 1–4*), three lung cancer cell lines (*Lane 5*, H69; *Lane 6*, U1285; *Lane 7*, U2020), and amplification product from a clonal *FHIT* cDNA.

have been able to examine the *FHIT* locus in detail, we find a correlation between deletions within *FHIT* and absence or aberration of *FHIT* RT-PCR products, as summarized in Table 3. We had suggested previously that aberrant RNAs may code for aberrant proteins with a dominant negative effect, but we have thus far found no evidence that the aberrant products are translated (see next section).

Because we believe that the aberrant RT-PCR products are, in most cases, indicators of the existence of an altered *FHIT* allele in some fraction of the cells examined, we have considered several reasons for the differences between our results and those of Thiagalingam *et al.* (7), who found, by unnested RT-PCR, a much lower frequency of aberrant RT-PCR products in colon carcinoma xenografts than we did by nested RT-PCR in a smaller sample of uncultured colon carcinomas. One possibility might be that primary colon tumors are heterogeneous for *FHIT* deletions and the subpopulations with *FHIT* deletions are not favored during xenograft growth. An explanation that we currently favor is that the aberrant transcripts are indeed present at a lower level than the apparent full length transcripts, being occasional transcripts from grossly altered *FHIT* alleles, and thus a single round of amplification may strongly favor amplification of the more prevalent transcripts from an uncrippled *FHIT* allele. In support of this interpretation is the fact that cancer cells that by Northern blot analysis look negative for *FHIT* expression, such as Kato 3, LoVo, CNE2, and CNE1 (for Northern analysis see Fig. 3 of Ref. 1), show aberrant RT-PCR products by nested RT-PCR as shown here for Kato 3 (Fig. 3*A*, *Lane 7*), LoVo (Fig. 3*A*, *Lane 6*), CNE1 (Fig. 3*A*, *Lane 3*), and CNE2 (Fig. 3*A*, *Lane 4*), which are very similar to the aberrant nested RT-PCR products previously observed in uncultured or cultured tumor cells of various cancer types (1, 4–6, 18). Also, obviously RT-PCR and nested RT-PCR could miss *FHIT* alleles with alterations in 5′ or 3′ exons, such as the RC48 *FHIT* alleles missing exons 8, 9, and 10.

Fig. 3*B* shows products of nested *FHIT* RT-PCR from lymphocyte DNA (Fig. 3*B*, *Lanes 1–4*) and some lung cancer cell lines without aberrant products (Fig. 3*B*, *Lanes 5–7*). Although the upper band in *Lane 2* has not been sequenced, it probably represents an insertion of some intron 4 sequence between exons 4 and 5, a phenomenon we have observed in amplifications from a number of lymphocyte DNAs.

Analysis of Fhit Protein in Cancer Cell Lines. Rabbit polyclonal antibody raised against the GST-Fhit fusion protein was used in immunoblot experiments to detect Fhit protein products in various cancer cell lines with and without homozygous deletions and/or aberrant RT-PCR products. Specificity of the antibody was determined by immunoblot analysis of protein extracted from Cos monkey kidney cells (Fig. 4*B*, *Lane 9*) or Cos cells transiently transfected with the pCMV-*FHIT*-Flag construct (Ref. 2; see Fig. 4, *A*, *Lane 1*, and *B*, *Lane 10*). Endogenous Fhit is strongly expressed by adenovirus 5 T-antigen-transformed human kidney cells 293 (Fig. 4, *A*, *Lane 4*, and *B*, *Lane 4*) and by normal kidney and kidney tumor cells passaged a few times in tissue culture (Fig. 4*B*, *Lanes 3* and *5*). As expected, cell lines with homozygous deletions of *FHIT*-coding exons, such as RC48, Kato 3, and AGS (Fig. 4, *A*, *Lanes 3* and *6*, and *B*, *Lane 6*) do not express Fhit protein. Additionally, Siha cells with loss but not complete absence of exon 5 and homozygous deletion in intron 4

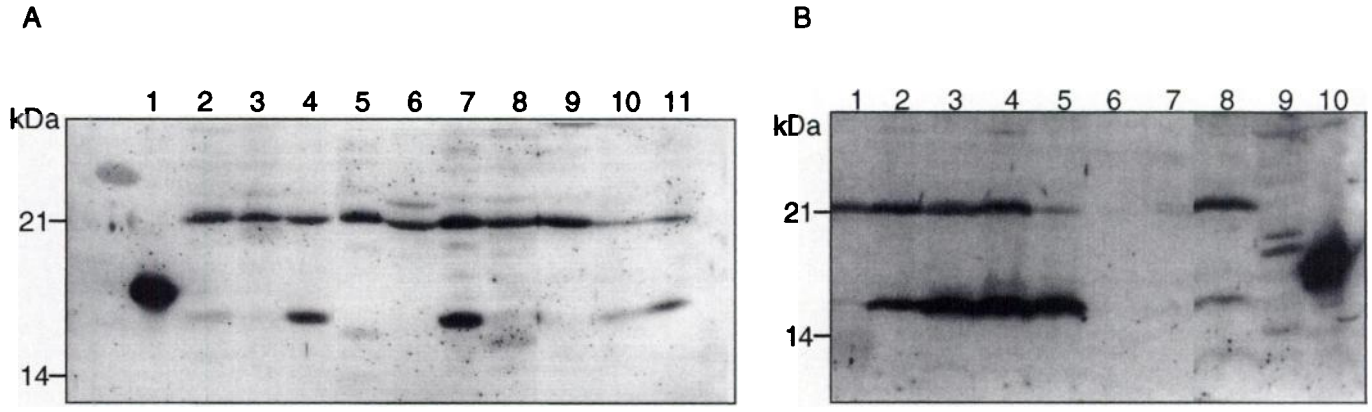

Fig. 4. Expression of Fhit in cancer cell lines. Lysates were prepared from normal and tumor cell lines, proteins were fractionated by PAGE and blotted to membranes, and the Fhit protein was detected using rabbit GST-Fhit antibody. *A*, detection of Fhit in lysates of Cos cells transiently transfected with the pCMV FHIT-Flag construct (*Lane 1*), RC49 (*Lane 2*), RC48 (*Lane 3*), 293 adenovirus 5 T antigen-transformed human kidney cells (*Lane 4*), JM human acute leukemia (*Lane 5*), Kato 3 (*Lane 6*), U2020 human lung carcinoma with homozygous deletion in chromosome region 3p12 (*Lane 7*), DT36 (*Lane 8*), Siha (*Lane 9*), HeLa (*Lane 10*), and Colo320 (*Lane 11*). Note that the antibody detects faint bands smaller than the M_r 17,000 endogenous Fhit in *Lanes 5* and *8*, containing protein from the JM leukemia and the DT36 laryngeal SCC. The exogenous Fhit-Flag protein (*Lane 1*) is larger than endogenous Fhit due to the octapeptide Flag epitope at the COOH terminus. *B*, demonstrates reproducible levels of expression in the cancer cell lines: DT36 (*Lane 1*; note smaller band), Colo320 (*Lane 2*), normal kidney cells at the third subculture (*Lane 3*), 293 (*Lane 4*), RCC at the third subculture (*Lane 5*), AGS (*Lane 6*), Siha (*Lane 7*), RC49 (*Lane 8*), Cos monkey kidney cells (*Lane 9*), and Cos/Fhit-Flag (*Lane 10*). These cell lines have been tested more than three times by Western blot with similar or identical results. Additional cells tested were breast cancer cell lines MDA-MB-231 (Fhit+), HBL100 (Fhit+), MDA-MB-436 (Fhit-); colon carcinoma cell lines RF1 (Fhit+) and RF48 (Fhit+) and GM607 lymphoblastoid cell line (Fhit++).

apparently do not express Fhit. Siha cells showed only abnormal *FHIT* RT-PCR product, so they may be like Kato 3 cells in having different deletions on the two *FHIT* alleles, such that all coding exons are present but each allele is missing a different coding exon. HeLa cells, which show near absence of exons 3 and 4, reproducibly show low expression of Fhit, suggesting that the HeLa aberrant allele, perhaps missing exons 3 and 4, is not translated; RC49 cells, which retain all *FHIT* exons but exhibit a rearranged exon 8 band, also appear to express a reduced level of Fhit (Fig. 4, *B*, *Lane 8*, and *A*, *Lane 2*), relative to the kidney cells in *Lanes 3–5* (Fig. 4*B*). Most interestingly, the DT36 cell line, for which homozygous deletion within *FHIT* was not observed, is apparently negative or nearly negative for Fhit expression (Fig. 4, *A*, *Lane 8*, and *B*, *Lane 1*), and both lanes show a suggestion of a lower band, which may react with Fhit antibody, as in the acute leukemia cell line JM (Fig. 4*A*, *Lane 5*). The RT-PCR product from DT36 cells exhibited a single RT-PCR product with an insertion of 40 bp between exons 4 and 5, and the JM cells have not been studied for integrity of the *FHIT* locus. The DT36 result strongly suggests that alteration to the 5′ untranslated region of *FHIT* can affect translation of the protein. The protein data suggest that even when DNA and RNA alterations of the *FHIT* locus have not been observed or the observed alterations are not in the protein-coding region, the Fhit protein may be absent, reduced, or possibly altered.

The complexity and heterozygosity of the DNA lesions observed within the *FHIT* locus by PCR and Southern blot analyses suggest that the types of alterations (deletions and/or rearrangements) observed in this locus may be different from deletions described in other potential tumor suppressor loci, possibly due to the fact that the *FHIT* gene encompasses the fragile 3B region. In fact, the two regions of *FRA3B* that have already been isolated as flanking sites to an HPV insertion or hybrid breakpoints (15, 16) occur within introns 4 and 5, respectively, surrounding the frequently deleted exon 5. Additionally, the AGS cell line, which appears to show a number of discontinuous homozygous deletions (see Table 2), clearly shows loss of a region including exon 3 and part of intron 3 encompassing the t(3;8). HeLa cells are nearly lacking the exon 3 and 4 *Bam*HI fragments, which flank the t(3;8) break, suggesting alteration to this region in a large fraction of HeLa cells. The fact that the HeLa cells appear to be heterogeneous, with some HeLa cells missing exon 3 and/or exon 4 and others retaining these exons, is surprising because HeLa cells have been in culture for many years and might be expected to be nearly clonal. For Kato 3 cells there is also a suggestion of heterogeneity and/or heterozygosity within the culture because exon 6 may be missing in some cells, whereas perhaps exon 5 is missing in others; *i.e.*, there may be two overlapping deletions in Kato 3 such that the two different *FHIT* alleles are both missing a common portion of intron 5, explaining the homozygous deletion, but missing different portions of the *FHIT* locus, such that there is no intact *FHIT* allele in any subpopulation, explaining the absence of Fhit protein. This type of heterogeneity was observed by FISH analysis using *FHIT* exon probes in early passage cultures of SCCs of the head and neck (18) and may suggest that absence of the Fhit protein does not necessarily confer a growth advantage in tissue culture. The fact that alterations in the *FHIT* gene have been observed in different regions of the locus, near exons 3 and 4, in intron 5 and in exons 8, 9, 10 (RC48, RC49) suggests that the *FHIT* gene is the target of loss and clonal expansion because if another single gene was the target, it would need to be spread over the same genomic region as the *FHIT* gene. The complexity of DNA lesions observed also suggests that it will be difficult to find a simple assay to detect the DNA lesions in cancer cell lines and extremely difficult to define lesions in uncultured tumor cells. Thus, the validity of the RNA assay is crucial. We have been able to correlate known DNA lesions with occurrence of aberrant RT-PCR products but to do the reverse for every aberrant RT-PCR product would not be possible. We are thus exploring the possibility of detecting altered RNAs by RNase protection studies. Alternatively, detection of the protein in uncultured tumors by immunohistochemistry may be the best way to assess the level of involvement of Fhit in various human cancers.

ACKNOWLEDGMENTS

We thank Michelle Ottey and Eric Snyder for skillful assistance in characterization of some of the *FHIT* cosmids.

REFERENCES

1. Ohta, M., Inoue, H., Cotticelli, M. G., Kastury, K., Baffa, R., Palazzo, J., Siprashvili, Z., Mori, M., McCue, P., Druck, T., Croce, C. M., and Huebner, K. The *FHIT* gene, spanning the chromosome 3p14.2 fragile site and renal carcinoma-associated t(3;8) breakpoint, is abnormal in digestive tract cancers. Cell, *84:* 587–597, 1996.
2. Barnes, L. D., Garrison, P. N., Siprashvili, Z., Guranowski, A., Robinson, A. K., Ingram, S. W., Croce, C. M., Ohta, M., and Huebner, K. Fhit, a putative tumor suppressor in humans, is a dinucleoside 5′, 5‴-P^1,P^3 triphosphate hydrolase. Biochemistry, *35:* 11529–11535, 1996.
3. Kastury, K., Baffa, R., Druck, T., Ohta, M., Cotticelli, M. G., Inoue, H., Negrini, M., Rugge, M., Huang, D., Croce, C. M., Palazzo, J., and Huebner, K. Potential gastrointestinal tumor suppressor locus at the 3p14.2 FRA3B site identified by homozygous deletions in tumor cell lines. Cancer Res., *56:* 978–983, 1996.
4. Sozzi, G. Veronese, M. L., Negrini, M., Baffa, R., Cotticelli, M. G., Inoue, H., Tornielli, S., Pilotti, S., De Gregorio, L., Pastorino, U., Pierotti, M. A., Ohta, M., Huebner, K., and Croce, C. M. The *FHIT* gene at 3p14.2 is abnormal in lung cancer. Cell, *85:* 17–26, 1996.
5. Sozzi, G., Alder, H., Tornielli, S., Corletto, V., Baffa, R., Veronese, M. L., Negrini, M., Pilotti, S., Pierotti, M. A., Huebner, K., and Croce, C. M. Aberrant *FHIT* transcripts in merkel cell carcinoma. Cancer Res., *56:* 2472–2474, 1996.
6. Negrini, M., Monaco, C., Vorechovsky, I., Ohta, M., Druck, T., Baffa, R., Huebner, K., and Croce, C. M. The *FHIT* gene at 3p14.2 is abnormal in breast carcinomas. Cancer Res., *56:* 3173–3179, 1996.
7. Thiagalingam, S., Lisitsyn, N. A., Hamaguchi, M., Wigler, M. H., Willson, J. K. V., Markowitz, S. D., Leach, F. S., Kinzler, K. W., and Vogelstein, B. Evaluation of the *FHIT* gene in colorectal cancers. Cancer Res. *56:* 2936–2939, 1996.
8. LaForgia, S., K., Morse, B., Levy, J., Barnea, G., Li, F., Cannizarro, L. A., Nowell, P. C., Glick, J., Boghosian-Sell, L., Weston, A., Harris, C. C., Drabkin, H., Patterson, D., Croce, C. M., Schlessinger, J., and Huebner, K. Receptor protein-tyrosine phosphatase gamma is a candidate tumor suppressor gene at human chromosome region 3p21. Proc. Natl. Acad. Sci. USA, *81:* 5036–5040, 1991.
9. Druck, T., Kastury, K., Hadaczek, P., Podolski, J., Toloczko, A., Sikorski, A., Ohta, M., LaForgia, S., Lasota, J., McCue, P., Lubinski, J., and Huebner, K. Loss of heterozygosity at the familial RCC t(3;8) locus in most clear cell renal carcinomas. Cancer Res., *55:* 5348–5353, 1995.
10. Genetics Computer Group. *Program Manual for the Wisconsin Package, Version 8*, Madison, WI: Genetics Computer Group, Madison, Wisconsin, 1994.
11. Lisitsyn, N. A., Lisitsina, N. M., Dalbagni, G., Barker, P., Sanchez, C. A., Gnarra, J., Linehan, W. M., Reid, B. J., and Wigler, M. H. Comparative genomic analysis of tumors: detection of DNA losses and amplification. Proc. Natl. Acad. Sci. USA, *92:* 151–155, 1995.
12. Lubinski, J., Hadaczek, P., Podolski, J., Toloczko, A., Sikorski, A., McCue, P., Druck, T., and Huebner, K. Common regions of deletion in chromosome regions 3p12 and 3p14.2 in primary clear cell renal carcinomas. Cancer Res., *54:* 3710–3713, 1994.
13. Wilke, C. M., Guo, S-W., Hall, B. K., Boldog, F., Gemmill, R. M., Chandrasekharappa, S. C., Bancroft, C. L., Drabkin, H. A., and Glover, T. W. Multicolor FISH mapping of YAC clones in 3p14 and identification of a YAC spanning both *FRA3B* and the t(3;8) associated with hereditary renal cell carcinoma. Genomics, *22:* 319–326, 1994.
14. Kastury, K., Ohta, M., Lasota, J., Moir, D., Dorman, T., LaForgia, S., Druck, T., and Huebner, K. Structure of the human receptor tyrosine phosphatase gamma gene (*PTPRG*) and relation to the familial RCC t(3;8) chromosome translocation. Genomics, *32:* 225–235, 1996.
15. Wilke, C. M., Hall, B. K., Hoge, A., Paradee, W., Smith, D. I., and Glover, T. W. FRA3B extends over a broad region and contains a spontaneous HPV16 integration site: direct evidence for the coincidence of viral integration sites and fragile sites. Hum. Mol. Genet., *5:* 187–195, 1996.
16. Paradee, W., Wilke, C. M., Wang, L., Shridhar, R., Mullins, C. M., Hoge, A., Glover, T. W., and Smith, D. I. A 350-kb cosmid contig in 3p14.2 that crosses the t(3;8) hereditary renal cell carcinoma translocation breakpoint and 17 aphidicolin-induced *FRA3B* breakpoints. Genomics, *35:* 87–93, 1996.
17. Rassool, F. V., Le Beau, M. M., Shen, M. L., Neilly, M. E., Espinosa, R., III, Ong, S. T., Boldog, F., Drabkin, H., McCarroll, R., and McKeithan, T. W. Direct cloning of DNA sequences from the common fragile site region at chromosome band 3p14.2. Genomics, *35:* 109–117, 1996.
18. Virgilio, L., Shuster, M., Gollin, S. M., Veronese, M. L., Ohta, M., Huebner, K., and Croce, C. M. *FHIT* gene alterations in head and neck squamous cell carcinomas. Proc. Natl. Acad. Sci. USA, *93:* 9770–9775, 1996.